Desalination and Water Treatment
www.deswater.com

doi: 10.5004/dwt.2019.23576

147 (2019) 20–30
April

High-flux electrospun polyvinyl alcohol microfiltration nanofiber membranes for treatment of oil water emulsion

Elham Karimi, Seyed Siamak Barekati, Ahmadreza Raisi*, Abdolreza Aroujalian

Department of Chemical Engineering, Amirkabir University of Technology (Tehran Polytechnic), Hafez Ave., P.O. Box 15875-4413, Tehran, Iran, Tel. +(9821) 64543125; Fax: +(9821) 66405847; email: raisia@aut.ac.ir (A. Raisi), Tel. +(9821) 64543290; emails: elhamkarimi2009@yahoo.com (E. Karimi), siamak.barekati@gmail.com (S.S. Barekati), Tel. +(9821) 64543163; email: aroujali@aut.ac.ir (A. Aroujalian)

Received 15 May 2018; Accepted 10 December 2018

ABSTRACT

In this work, a novel class of high-performance microfiltration membranes consisting of an electrospun polyvinyl alcohol (PVA) nanofiber top layer and a nonwoven polyester support was developed. To achieve water-insoluble PVA nanofiber membranes, two different cross-linking methods were used: (1) chemical cross-linking using citric acid as a cross-linking agent and subsequent thermal treatment of the prepared electrospun nanofibers and (2) photo-cross-linking of an ultraviolet (UV)-curable PVA polymer that was synthesized by adding C=C bonds to PVA. Effects of citric acid concentration on membrane properties and separation performance were investigated. The separation performance and antifouling properties of the membranes were studied for microfiltration treatment of an oil/water emulsion. The results showed that more concentration of citric acid in the specimens led to a lower swelling degree. The use of citric acid in combination with UV irradiation had a synergistic effect in the cross-linking reaction. The UV cross-linked electrospun membrane had uniform and finer fibers, which resulted in a membrane with small pore size and high porosity, while the chemical cross-linking reaction occurred between the polymer fibers and the fibers fused together during thermal treatment. Meanwhile, the most striking characteristic of the photo-cross-linked PVA nanofiber membranes was its high durability and mechanical strength.

Keywords: Polyvinyl alcohol membrane; Photo-cross-linking; Electrospinning; UV irradiation; Oil/water emulsion

1. Introduction

Electrospun nanofiber membranes based on polyvinyl alcohol (PVA) can be one of the most interesting membranes among researchers and industries due to the vast advantages of PVA, such as its high electrospinability, inherent adhesiveness, high hydrophilicity, high water permeability, and antifouling potential [1]. Nevertheless, the high solubility of PVA in water is the biggest obstacle for the use of this unique polymer in the fabrication of membranes, which are going to be used for aqueous applications or even for circumstances with relatively high moisture. To address this, the PVA should be adequately cross-linked through the consumption of OH groups responsible for its highly polar nature [2]. Hence, a vast majority of researches have been done to manipulate and modify this polymer. In addition to the traditional methods of PVA cross-linking such as freeze-thaw inducement of crystallization, heat treatment, and chemical cross-linking, photo-cross-linking through incorporating either photosensitive bands or photo-reactive nanoparticles to the polymer is a novel cost-effective and time-efficient method, which is very suitable for heat-sensitive materials and pharmaceutical products [3]. This novel method has been examined not only on PVA but also on some other polymers [4–7].

In the photo-cross-linking technique, a component with an unsaturated double-bond group like *l*-methyl-4-

* Corresponding author.

[2-(4-formylphenyl)-ethyl]-pyridinium-methosulfate (SbQ-4) [8], thionyl chloride [9], and acryloyl chloride [3,10] was added to the PVA through a chemical reaction to obtain an ultraviolet (UV)-curable polymer. Then the UV irradiation was applied during the electrospinning process or after preparation of the nanofibers in order to cross-link the electrospun nanofibers. Zeng et al. [9] used thionyl chloride for the synthesis of the UV-curable PVA derivative. They prepared photo-cross-linked PVA nanofibers by exposing the electrospun nanofibers to UV irradiation. In another study [3], photo-reactive bonds of the C=C were added to the PVA by reaction with acryloyl chloride. Afterward, the product of reaction was dissolved in water for preparing a highly sensitive solution. A layer of PVA nanofibers was prepared by electrospinning, and this layer was exposed to the UV irradiation for photo-cross-linking. Lyoo et al. [4] electrospun the blend fibers of poly(vinyl cinnamate)/poly(3-hydroxybutyrate-co-3-hydroxyvalerate) from chloroform solutions, and subsequently, the nanofibers were cross-linked via UV irradiation as a complementary stage. The photo-cross-linking of the electrospun nanofibers can be performed during the electrospinning process. Gupta et al. [5] synthesized the functionalized poly(methyl methacrylate-co-2-hydroxyethyl acrylate) with the cinnamate functional group through an esterification reaction between the hydroxyl group of 2-hydroxyethyl acrylate and cinnamoyl chloride. Then the cross-linked electrospun nanofibers were prepared by simultaneous electrospinning and UV irradiation. Zeytuncu et al. [10] also prepared photo-cross-linked PVA nanofibers containing thioamide groups by a simultaneous electrospinning process and UV irradiation.

Recently, Karimi et al. [11] used the photo-reactive nanoparticles like TiO_2 to prepare the photo-cross-linked electrospun PVA nanofiber membranes by a simultaneous electrospinning process and UV irradiation. They investigated the effect of UV irradiation conditions on the surface properties and separation performance of the prepared membranes in the microfiltration of the oil/water emulsions. The main goal of the present work is to prepare the photo-cross-linked electrospun PVA nanofiber membranes by incorporating C=C bonds in the backbone of PVA to synthesize a UV-curable polymer and by simultaneous electrospinning and UV irradiation. The separation performance of the prepared photo-cross-linked membrane was compared with the chemically cross-linked PVA membranes containing different amounts of cross-linking agent for the treatment of oily wastewater. The morphological, mechanical, and antifouling properties of the prepared electrospun membranes were characterized by the scanning electron microscopy (SEM), Fourier transform infrared (FTIR), swelling degree, and mechanical tests as well as by the membrane fouling analysis.

2. Materials and methods

2.1. Materials

PVA (>98% hydrolyzed) with the molecular weight of 72,000 g/mol as the main material in the membrane electrospinning solution, citric acid as the cross-linking agent, Triton X-100, acryloyl chloride, and *N*-methylpyrridine (NMP) were used as received from Merck Co. Ltd. (Darmstadt, Germany) without further purification. Darocur®1173 as the photo-initiator was purchased from Sigma-Aldrich (MO, USA). The gas oil and deionized water were used for the preparation of oil/water emulsion.

2.2. Preparation of the chemically cross-linked PVA nanofiber membrane

The chemically cross-linked nanofiber membrane was prepared according to the procedure previously described by Karimi et al. [11]. Briefly, 10%wt. PVA was dissolved in water at 90°C, and the specific amounts of citric acid were added to the solution and stirred for 6 h at the same temperature, and then the heater was turned off for the next 24 h. One hour prior to the electrospinning process, 0.6%wt. Triton X-100 was added into the polymer solution under vigorous stirring. The obtained solution was loaded into a syringe attached to an electrospinning apparatus (Nanomeghias, Tehran, Iran), and it was stymied into the pump 12 cm far from the collector. A layer of nonwoven polyester was placed on the collector as the membrane support layer. The flow rate of the solution exodus from the needle was 2 mL/min, and the high DC voltage was adjusted at 22 kV as well. Finally, the obtained PVA nanofiber membrane was cross-linked by heating at 150°C for 5 min. The prepared electrospun nanofiber membranes were named as indicated in Table 1. The schematic of the chemical cross-linking reaction is depicted in Fig. 1.

Table 1
The prepared electrospun PVA nanofiber membranes

Membrane	PVA concentration (%wt.)	Citric acid concentration (%wt.)	UV irradiation
M1	10	5	–
M2	10	10	–
M3	10	15	–
M4	10	10	√

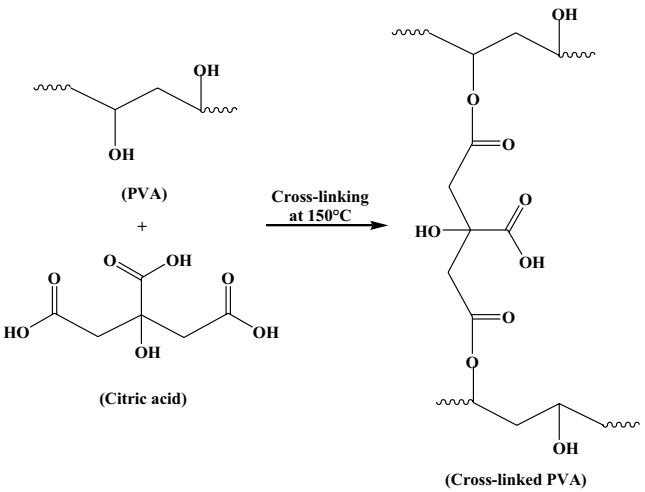

Fig. 1. The schematic of the chemical cross-linking reaction.

2.3. Preparation of UV cross-linked PVA nanofiber membrane

In order to prepare the UV cross-linked PVA nanofiber membrane, the following procedure was used for synthesis of the PVA-based UV-reactive polymer by adding a UV-sensitive band to the PVA molecules:

- Ten grams of PVA was added to 200 mL of NMP and dissolved at 110°C for 2 h. Then the obtained solution was cooled to room temperature for 2 h.
- A 0.5 mL of acryloyl chloride was slowly added to the prepared polymer solution dropwise, and the solution was vigorously stirred for 1 h.
- The UV-reactive PVA polymer was obtained by pouring the solution in 1 L of methanol at 0°C.
- Finally, the precipitated polymer was put under vacuum for 3 discontinuous 12-h periods for removing the residual solvent.

All the procedures should be carefully done in a dark room because the prepared polymer is photosensitive. The schematic of the procedures for preparing the UV-PVA polymer is depicted in Fig. 2.

A 10%wt. of the UV-reactive PVA polymer and 10%wt. citric acid were dissolved in deionized water at 85°C and stirred for 1 h. Afterward, the heater was turned off for cooling the solution to ambient temperature. Subsequently, 0.6%wt. Darocur®1173 and the same amount of Triton X-100 were poured into the solution, distinctly 1 h prior to electrospinning. The homogeneous electrospun solution was fed to the electrospinning apparatus in which the nanofibers were exposed to a 200 W UV lamp parallel to the nanofibers' path between the nozzle and the collector. The other electrospinning conditions were similar to those for the chemically cross-linked nanofiber membranes. This photo-cross-linked nanofiber membrane was named M4.

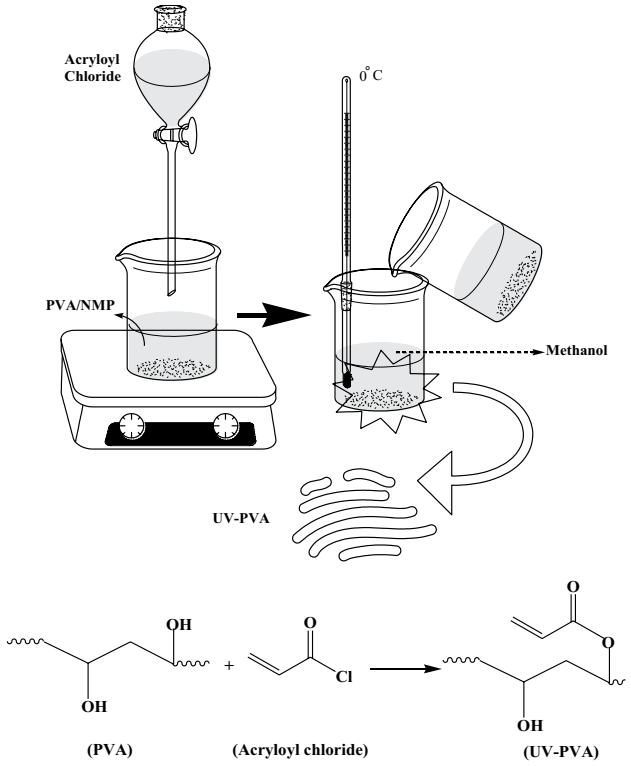

Fig. 2. The schematic of the procedure for preparing the UV-PVA polymer.

2.4. Preparation of oil/water emulsion

The oil/water emulsion is a stable system consisting of tiny droplets of oil dispersed in water. In this study, stable oil/water emulsions with 3,000 ppm oil concentration were prepared by dispersion of gas oil in water in the presence of 3,000 ppm Tween-80 as emulsifier by a homogenizer (WiseTis-HG-15D, Daihan Co., South Korea) at 12,000 rpm for 1 h.

2.5. Characterization tests

The morphology and structure of the prepared membranes were investigated using a SEM apparatus (AIS2100, Seron Technologies Inc., South Korea) after coating a thin layer of gold on the surface of each membrane sample.

The existing functional groups in the structure of polymers were detected by an FTIR spectroscopy (Nicolet Instrument Co., Madison, WI, USA) with the resolution of 4 cm^{-1} over a wave number range of 4,000–600 cm^{-1}. The area of samples used in each test was 4 cm^2.

The swelling degree of the prepared electrospun membranes was determined by the gravimetric method and calculated using the following equation [12]:

$$\mathrm{SD}(\%) = \left(\frac{W_w - W_d}{W_d}\right) \times 100 \tag{1}$$

where W_d and W_w are the membrane weight before and after soaking in the deionized water for 48 h.

The mechanical properties including tensile strength, tension ratio, and subsequently the elastic module of the membrane were also determined for various prepared membranes. The membrane samples were cut into 5 mm × 20 mm dimensions and placed in a tensile strength tester machine (AI-3000, Gotech Testing Machines Inc., Taichung, Taiwan). Then the machine started the test with a typical cross-head speed of 2 mm/min at room temperature. The thickness of all the samples was ~110 μm.

The inner contact angles between the curvature surface of the water droplet and the membrane samples were calculated by analyzing photos which were taken from the surface of the membrane, where a 5-μL water droplet was put on the membrane surface by a microsyringe. To minimize the experimental error, the contact angle was measured at several locations of the membrane surface and the average values were reported.

The mean pore diameter of the prepared electrospun membranes was estimated using the following equation [13]:

$$D_p = \sqrt{\frac{32(2.9 - 1.75\varepsilon)\eta\delta Q}{\varepsilon A \Delta P}} \tag{2}$$

where D_p is the mean pore diameter, η is the water viscosity at room temperature (Pa·s), δ is the membrane thickness (m),

Q is the permeate flow rate of pure water (m^3/s), ε is the bulk porosity, A is the membrane area (m^2), and ΔP is the operating pressure (MPa).

The bulk porosity of the electrospun membrane was calculated through the following equation:

$$\varepsilon = \frac{W_w - W_d}{\rho A \delta} \tag{3}$$

where w_w and w_d are the membrane weight (g) in wet and dry states, respectively, and ϱ is the water density at room temperature (g/m^3).

The separation performance of the prepared electrospun PVA membrane was investigated by the microfiltration of the pure water and oil/water emulsion using a cross-flow membrane module at 1.5 bar and room temperature. The schematic of the cross-flow microfiltration setup used in the experiments is presented in Fig. 3. By weighing the collected permeate during a specific time, the permeate flux was calculated by the following equation:

$$J = \frac{W}{At} \tag{4}$$

where J is the permeate flux, W is the weight of collected permeate, and t is the time duration of the experiments.

Furthermore, the oil concentrations in the feed and permeate were measured using the chemical oxygen demand (COD) test according to the 5220D standard method [14]. The COD of solutions was measured at the wavelength of 600 nm by a UV-Vis spectrophotometer (Hitachi U-2001 UV-Vis spectrophotometer, Hitachi, NJ, USA). Meanwhile, the oil rejection was calculated through the following equation:

$$R(\%) = \left(1 - \frac{C_p}{C_f}\right) \times 100 \tag{5}$$

where R is the oil rejection and C_f and C_p are the concentrations of oil in the feed and permeate streams, respectively.

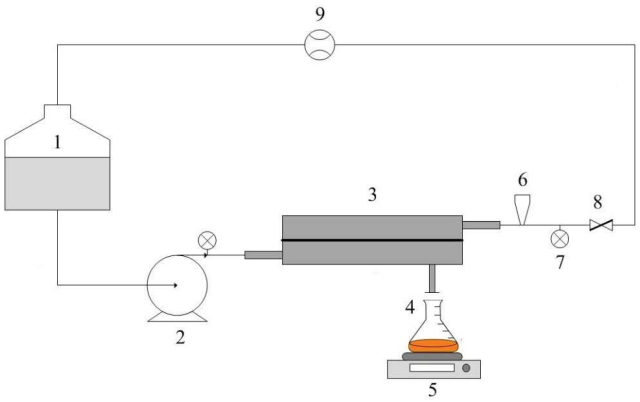

Fig. 3. The schematic of the cross-flow microfiltration setup (1: Feed tank, 2: Feed pump, 3: Membrane module, 4: Permeate, 5: Digital balance, 6: Pressure controller, 7: Pressure gauge, 8: Regulating valve, 9: Flow meter).

2.6. Evaluation of membrane fouling

In order to evaluate the antifouling property of the prepared electrospun membranes during the microfiltration of the oil/water emulsions, the flux decrease ratio (FDR) and the mass transport resistances were determined for various membranes. The FDR, as a measure of the membrane fouling, was calculated by determining the initial oil/water flux and final steady-state oil/water flux during the microfiltration test as follows:

$$\mathrm{FDR}(\%) = \left(1 - \frac{J_{of}}{J_{oi}}\right) \times 100 \tag{6}$$

where J_{of} is the final steady-state oil/water flux and J_{oi} is the initial steady-state oil/water flux.

The total mass transport resistance against the permeation through the membrane consists of three resistances, i.e. membrane resistance, fouling resistance, and cake resistance [15]. The membrane resistance that represents the intrinsic resistance of the membrane against the feed components transport through the membrane is determined by the microfiltration of pure water through the virgin membrane:

$$R_m = \frac{\rho \Delta P}{\eta J_{wv}} \tag{7}$$

where R_m is the intrinsic resistance of the membrane, ρ and η are the density and viscosity of the permeate stream, respectively, ΔP is the operating pressure, and J_{wv} is the pure water flux of the virgin membrane.

The fouling resistance indicates the mass transport resistance due to the membrane fouling by blocking of the membrane pores and irreversible adsorption of the oil droplets on the surface and wall of the pores. This resistance is determined by the microfiltration of pure water through the fouled membrane:

$$R_f = \frac{\rho \Delta P}{\eta J_{wf}} - R_m \tag{8}$$

where R_f is the fouling resistance and J_{wf} is the pure water flux of the fouled membrane.

The cake resistance is the mass transport resistance due to accumulation of the oil drops on the surface of the membrane and formation of a cake/gel layer. This resistance is calculated by the following equation:

$$R_c = \frac{\rho \Delta P}{\eta J_{of}} - R_m - R_f \tag{9}$$

where R_c is the cake resistance.

3. Results and discussion

3.1. Characterization of membranes

The SEM images from the top surface of various prepared electrospun PVA membranes are presented in Fig. 4. A comparison between SEM images of the UV cross-linked PVA

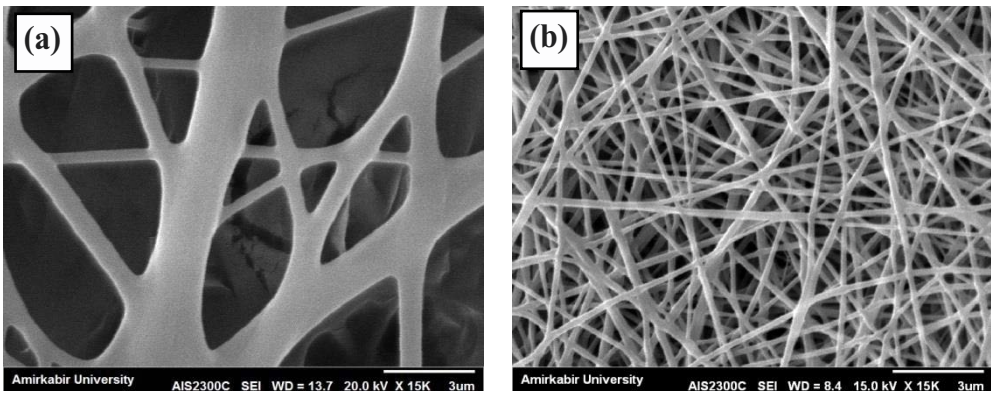

Fig. 4. The SEM images from the top surface of various prepared electrospun PVA membranes: (a) M2 and (b) M4.

membrane and the chemically cross-linked one revealed that the UV cross-linked electrospun membrane had uniform and finer fibers. The mean fiber diameter for the M4 membrane sample was about 136 nm, whereas the mean fiber diameter for the M2 membrane sample was 531 nm. Another noteworthy result extracted from the SEM analysis is that the fibers of the UV cross-linked membrane are more uniform in diameter than those of the chemically cross-linked PVA membrane. In other words, the difference between the diameter of the smallest and the largest fibers of the UV-PVA membrane was about 149 nm. On the contrary, this value for the chemically cross-linked PVA membrane (M2 sample) was about 2,047 nm. The finer and uniform fibers of the UV cross-linked electrospun membrane can be attributed to the lower glass transition temperature of the UV-PVA polymer and lower viscosity of the UV-PVA solution. Generally, a polymer with lower glass transition temperature has finer fibers that will be scaffolded from it through the electrospinning process [16]. Furthermore, as the viscosity of the PVA/citric acid solution is enormously higher than the viscosity of UV-PVA solution, its corresponding nanofibers are thicker than the UV-PVA nanofibers [9]. Additionally, Fig. 4(a) shows that in the chemically cross-linked nanofibers, the cross-linking reaction occurred between the polymer fibers and the fibers fused together during thermal treatment.

Fig. 5 indicates the FTIR spectra of the uncross-linked, chemically cross-linked, and photo-cross-linked PVA membranes. All the groups observed in the FTIR spectra of the nanofiber membranes are listed in Table 2. The CH_3 symmetrical deformation mode is identified by peaks at 1,383 and 1,467 cm^{-1}. The vibrational band observed in the range of 2,850–3,000 cm^{-1} is an indication of C–H stretching of the alkyl groups [17]. The detection of C=C in the spectra of the UV cross-linked membrane sample underlines the fact that the efficiency of the photo-cross-linking reaction is not 100%, in the sense that during the UV irradiation some of the vinyl bonds did not break down. This is an indisputable fact that has been observed by some researchers, namely, Xu et al. [18] had a similar observation in their work as they found that all double bonds are not consumed in the cross-linking reaction. There is a core problem with this event. Despite this bond being very photosensitive, the time nanofibers were exposed to the UV beams during their travel to the collector is very short. In this reaction, the unstable vinyl bonds have a penchant for converting to stable ones by breaking down to free radicals and subsequently forming covalence bonds. The required energy for this reaction is supplied by the UV beams expeditiously. Meanwhile, the detected peak in the range of 1,760 cm^{-1}, which is attributed to the C–O–Cl bond, clearly highlights the presence of acryloyl chloride in the reaction

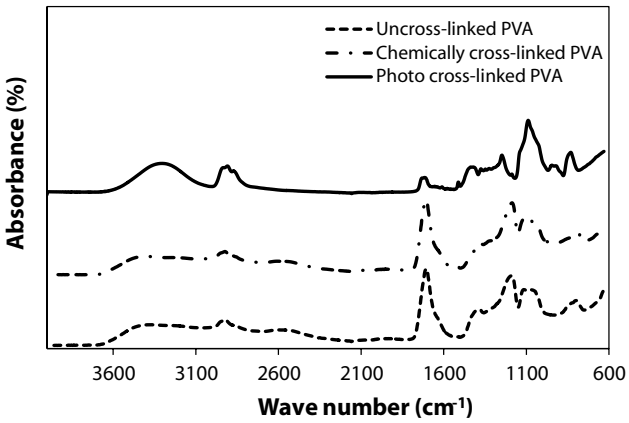

Fig. 5. The FTIR spectra of the uncross-linked, chemically cross-linked, and photo-cross-linked PVA membranes.

Table 2
The observed absorption bands in the FTIR spectra of various PVA nanofiber membranes

Bond	Wave number (cm^{-1})
C–H (Rocking)	820–870
CH_3 (symmetrical deformation mode)	1,383 and 1,467
C–O–C	1,050–1,150
C–C (Stretching vibration)	1,100–1,300
OH (Alcohol, bending vibration)	1,490–1,600
C–O (Stretching vibration)	1,700–1,725
C–O–Cl	1,760
C–H (Stretching vibration)	2,850–3,000
O–H (Carboxyl, stretching vibration)	2,500–3,300
OH (Alcohol, stretch, H-bonded)	3,200–3,600
OH (Alcohol, stretch, free)	3,500–3,700

environment. Another exquisite point to be mentioned is that the intensity of OH groups after either photo-cross-linking or chemical cross-linking reaction in the samples was decreased. It is also important that in the photo-cross-linking reaction, the presence of citric acid and photo-reactive bonds have a synergistic effect on the progression of the reaction, which means they are complementary of each other. In the UV-cured PVA nanofiber membrane, not only do the UV-reactive bands readily induce by UV irradiation due to their strong aspiration to breaking down and convert to free radicals to form new stable bonds with the chains in their vicinity but also the cross-linking agent significantly contributes to the reaction. The lower intensity of the hydroxyl bond in the UV cross-linked sample in comparison with the uncross-linked PVA sample approves this effect. At the other extreme, the chemically cross-linked nanofiber membranes formed their covalent bonds through the ensuing reaction shown in Fig. 1. The broad peak in the range of 3,200–3,550 cm^{-1} refers to –OH intermolecular and intramolecular hydrogen bonding. In the esterification reaction between –OH in PVA and –COOH in citric acid, whereupon PVA is cross-linked, the chains lose their hydroxyl groups. This reaction is a good explanation for decreasing the intensity of the hydroxyl bond as shown in Fig. 5.

PVA is a hydrophilic polymer due to the hydroxyl group it possesses. In fact, PVA is inclined to adsorb water forcefully through its hydroxyl pendant groups. The cross-linking reaction is a way to hinder PVA from dissolving in aqueous environments. Although cross-linked PVA can withstand dissolving in water, it is plausible that this reaction would be carried out incompletely and the membrane would absorb water. There is a mutual relationship between the swelling degree and solubility. In other words, the increment in the solubility leads to enhancement in the swelling degree and vice versa. The swelling degree is an estimation of the weight of water uptake per weight of the nanofiber membrane [19]. Hence, the swelling degree is a convincing representative of cross-linking degree [20]. The results of the swelling test are listed in Table 3. The swelling experiments prove that the M4 membrane sample had the least water uptake. This underlines the fact that the proposed photo-cross-linking reaction is an efficient method for modifying PVA. By comparing the corresponding results of the chemically cross-linked nanofiber membranes, it is found that the more cross-linked membrane has a lower swelling degree. This means that the M3 membrane sample successfully remains almost unchanged in water for 2 d. The swelling degree for the chemically cross-linked membranes is in the order of M1 > M2 > M3. This means that the swelling degree of the chemically cross-linked PVA membranes is decreased by an enhancement in the cross-linker concentration. A similar conclusion has been reported by other researchers, namely, Gohil and Ray [21] examined different concentrations of maleic acid for investigating the cross-linking degree and proved that the cross-linking degree has a direct relationship with the maleic acid concentration. Generally, the polymer swelling is a function of the cross-linking degree, polymer chain length, surface area, and porosity. In the case of PVA membrane, the swelling degree depends upon the availability of the number of hydroxyl groups and mobility of PVA chains [22]. Higher cross-linker concentration leads to a higher cross-linked polymer and vice versa for a lower cross-linker concentration [21] because enough citric acid molecules are present for the cross-linking reaction at higher cross-linker concentrations. As previously mentioned, the higher cross-linked membrane has a lower swelling degree. This is mainly because of the lower cross-linked polymers that have longer chain length and are easy to expand. In contrast, the chain length in the higher cross-linked polymers is smaller and difficult to swell. Moreover, the higher number of hydroxyl groups attracts a large number of water molecules. The absorbed water occupies the empty spaces between the polymer chains and displaces them, thus resulting in the swelling. Once the chains are cross-linked, they have little mobility relative to each other and hence the incoming water cannot make space for itself, restricting the number of water molecules absorbing into the PVA membrane [23]. The polymer cross-linking hence performs a dual role in controlling water absorption: it reduces the number of hydroxyl groups and limits the movement of the polymer chains by covalently linking them. Both of these lead to the reduction of water absorption and hence reduction in the membrane swelling. Likewise, the surface area and porosity of a polymer are tunable by changing the physicochemical parameters. High surface area and porosity also encourage the polymer swelling.

Table 3
The values of swelling degree, contact angle, porosity, and mean pore size of various prepared membranes

Membrane	Degree of swelling (%)	Contact angle (°)	Porosity (%)	Mean pore size (nm)
M1	43	32.1 ± 1.2	89	333.8
M2	28	35.4 ± 1.7	82	313.2
M3	25	37.1 ± 2.0	74	232.8
M4	16	32.3 ± 1.3	93	101.0

The values of the water contact angle, porosity, and pore size of different electrospun PVA membranes are provided in Table 3. It can be seen that the porosity of the prepared electrospun membranes is high. For the chemically cross-linked membranes, the bulk porosity decreased as the concentration of the cross-linking agent enhanced. Based on the results of SEM analysis, the cross-linking reaction occurred between the polymer fibers and the fibers fused together during the thermal treatment and led to thicker fibers. Thus, the membrane porosity decreased from 89% to 74% by increasing the citric acid concentration from 5%wt. to 15%wt. Moreover, the high porosity of the photo-cross-linked electrospun PVA membrane can be attributed to its narrow fibers. Furthermore, Table 3 shows the mean pore size of the membrane which was measured by the filtration velocity method using the Guerout–Elford–Ferry equation [13]. It can be seen that the photo-cross-linked electrospun PVA membrane (M4 sample) had smaller pore size than the chemically cross-linked membranes because of its narrow fibers. Likewise, the mean pore sizes of the M2 and M4 membrane samples were determined from the SEM image analysis using the Image J software, and the mean pore sizes of 320 and 116 nm were found for the M2 and M4 membranes, respectively.

As indicated in Table 3, the water contact angle of the chemically cross-linked PVA membranes was slightly

enhanced by increasing the citric acid concentration. This implies that the membrane hydrophilicity slightly decreased. As shown in Fig. 1, in the esterification reaction between –OH in PVA and –COOH in citric acid, whereupon PVA is cross-linked, the chains lose their hydroxyl groups and the cross-linking reaction further proceeds as the concentration of the cross-linking agent increases. Therefore, the membrane hydrophilicity reduced by consuming the hydroxyl groups during the cross-linking reaction.

The values of tensile modulus, tensile strength, and elongation to break ratio of various prepared nanofiber membranes are given in Table 4. As observed in this table, the tensile strength and elongation ratio are contradicting with each other. An increase in the tensile strength shows the increase in the brittleness, and an enhancement in the elongation shows the increase in ductility of the material. Thus, the usual trade between the tensile strength and elongation is that one grows while the other decreases. Also, a comparison between the chemically cross-linked membranes (M1, M2, and M3 samples) and the UV-cured membranes (M4 sample) indicates that the M4 sample had lower tensile strength and higher elongation ratio. As mechanical behavior severely undergoes a chemical structure [24], the changes occurring on the main chain and side chains on PVA to form UV-PVA can cause differences between T_g of these two polymers. It is well known that a decrement in the T_g of the polymers leads to a higher mobility; in fact, in lower T_g, the segments can rotate along the main chain freely. This means that a polymer with lower T_g exhibits a greater elongation compared with a rigid polymer, under lower applied force. In other words, this is a clear-cut reason and a good explanation for the different mechanical behavior of the M4 membrane from other membranes. Another reason for the different mechanical behavior of the UV-cured membrane from the chemically cross-linked membranes is the difference between the preparation methods for these electrospun membranes. The SEM image of the M4 membrane (Fig. 4(b)) shows that the polymer fibers independently collected on the substrate during the preparation of the UV-cured membrane and resulted in an electrospun membrane with thinner fibers. On the other hand, the SEM image of the M2 membrane (Fig. 4(a)) reveals that when the cross-linking reaction chemically occurs, not only the polymer chains are connected to each other but also the fibers are connected together, and this leads to thicker polymer fibers. This implies that a nanofibrous membrane with fused fibers exhibits a greater tensile strength and a lower elongation ratio compared with a membrane with narrow fibers. Moreover, the differences in the mechanical behavior of the M1, M2, and M3 membrane samples are due to the differences in the cross-linking degree. Generally, a cross-linked PVA has a firm three-dimensional construction of chains connected together by a covalence bond [25]. As the cross-linking degree increases, these covalence bonds will be invigorated [26]. As previously mentioned, the swelling degree is a representative of the cross-linking degree due to the direct relationship it has with the cross-linking degree. Thus, as the swelling degree increases, mobility decreases. In the same vein, elongation ratio decreases from M1 to M3, as the swelling degree decreases. On the contrary, in this route, the tensile strength reduces due to the increase in rigidity.

Table 4
The values of tensile strength and elongation to break ratio of various prepared membranes

Membrane	Tensile strength (MPa)	Elongation ratio (%)
M1	98.56	256.56
M2	138.97	194.66
M3	169.59	153.52
M4	1.903	271.55

3.2. Separation performance of membranes

The size of oil emulsion droplets in the feed solution was measured by a laser diffraction particle size analyzer (Nano ZS (red badge), ZEN3600, Malvern Co., UK). The droplet size distribution of the oil in water emulsion with oil concentration of 3,000 ppm is presented in Fig. 6. As observed, the mean size of the oil droplet is about 901 nm.

The time dependency of the pure water flux and oil/water flux for various prepared electrospun PVA membranes is shown in Fig. 7. It is observed that both water and oil/water fluxes of the M4 membranes are lower than those of the chemically cross-linked membranes. The permeation fluxes for the chemically cross-linked membranes decrease in the order of M1 < M2 < M3. The observed trends for the pure water and oil/water fluxes can be related to the pore size, porosity, hydrophilicity, and swelling degree of the membranes. The photo-cross-linked PVA membrane had lower permeation flux because of its lower mean pore size and the swelling phenomenon. In the swelling phenomenon, the water molecules accumulate between the polymer chains and increase the free volumes in the membrane matrix, consequently increasing the permeation flux. In fact, more cross-linked membranes have lower swelling degree that results in lower water and oil/water fluxes.

Furthermore, as indicated in Fig. 7(b), a sharp oil/water flux decline occurred during the early period (up to 20 min) of microfiltration, followed by smooth flux decay in the time interval of 20–40 min and then approached a steady-state limit after 40 min. The flux decline during the microfiltration of the oil/water emulsion is an indication of the membrane fouling due to pore blocking by small oil droplets, deposition of the oil drops on the membrane surface, and formation of a gel layer on the membrane surface. As the feed stream passes over the membrane surface, the small oil droplets enter the membrane pores and might deposit on the surface and wall of the pores, while most of the oil drops separate from the bulk feed solution due to their larger size than the membrane pore size and accumulate on the membrane surface. The blocking of the membrane pores and the formation of the viscous gel layer on the membrane surface are responsible for the additional resistances toward the mass transport through the membrane in addition to the membrane resistance and result in the flux decline during microfiltration with the prepared electrospun PVA membranes. Similar observations in the previous studies [11,27–30] were reported for the filtration of oil/water emulsions and oily wastewater by different polymeric membranes. Moreover, a comparison between the oil/water flux of the chemically cross-linked membranes (M1, M2, and M3 membranes) and the UV-cured membrane (M4

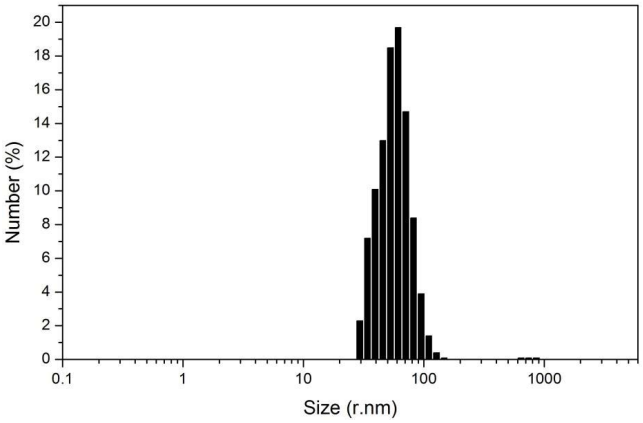

Fig. 6. The size of oil emulsion droplets in the feed solution.

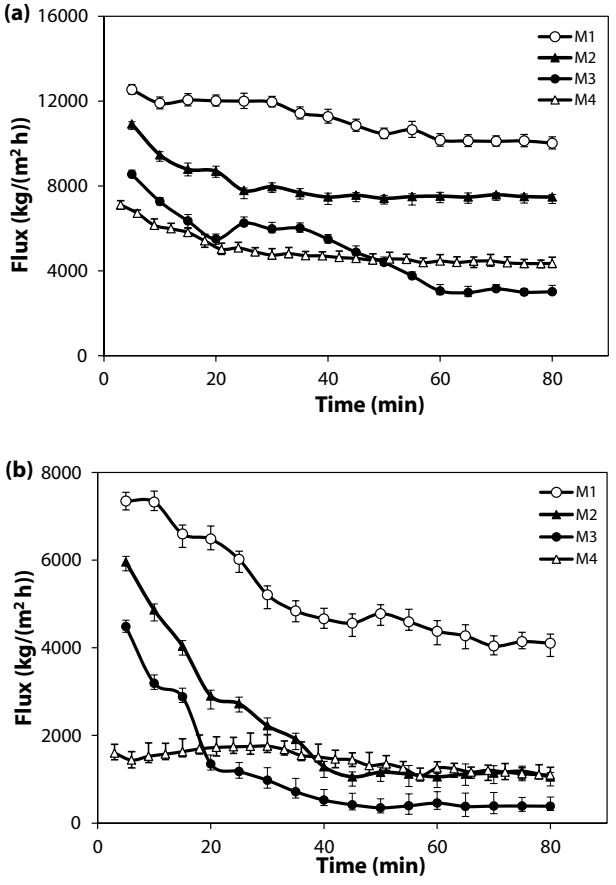

Fig. 7. The pure water flux (a) and oil/water flux (b) of the prepared electrospun PVA nanofiber membranes as a function of time.

membrane) indicates that the oil/water flux of the M1, M2, and M3 membrane samples rapidly decreased at the early period of the filtration due to the membrane pore blocking by the small oil droplets, while the oil/water flux of the M4 sample is almost constant. This means that the membrane pore blocking by the small oil droplets is more severe for the chemically cross-linked membranes due to their larger pore sizes. As presented in Table 3, the M1, M2, and M3 membranes had a larger pore size; therefore, more small oil droplets enter the pores of these membranes and might deposit on the surface and wall of the pores, consequently sharply reducing the permeate flux at an early period of filtration.

The values of oil rejection for the prepared membranes are shown in Table 5. The M2, M3, and M4 membrane samples had an oil rejection higher than 99%, which implies that these membranes can successfully separate the oil/water emulsions. It is also found that those membranes suffering from the high swelling degree show a poor performance in terms of oil rejection. This means that by increasing the swelling degree, the pore size will consequently increase, providing a wider route for the oil droplets to convey readily. At the other extreme, these wide routes provide a chance for membranes to have higher flux as well. Nevertheless, as the tortuosity is very high for the electrospun membranes, their rejection is much higher than the other types of membranes. High tortuosity inhibits the oil droplets from convection to the other side of the membrane.

Finally, the separation performance of the prepared electrospun PVA nanofiber membranes was compared with the performance of different electrospun membranes reported in the literature for the separation of oil/water emulsions, and the results are given in Table 5. It can be seen that the oil/water flux and rejection of the electrospun PVA membranes prepared in this study are higher than those of the membranes reported in the literature. For example, the M2 and M4 membranes have the final steady-state flux of 1,118.1 and 1,163.3 kg/(m^2 h) and oil rejection of 99.4% and 99.8% for the separation of a 3,000 ppm oil/water emulsion.

3.3. Antifouling performance of membrane

Although the fouling tendency of a membrane is affected by the hydrodynamic conditions of the filtration process [35], the fouling tendency of the prepared electrospun membranes was studied experimentally and calculated based on Eqs. (6)–(9). Antifouling properties of the membranes in terms of the FDR and mass transport resistances are presented in Table 6. In this study, the FDR, as an indication of the fouling tendency of the membrane, was calculated based on Eq. (6). The greater FDR value shows the higher fouling tendency of the membrane. The FDR values for different membranes indicated that the M1 membrane sample had the lowest FDR value between the chemically cross-linked PVA membranes due to the highest hydrophilicity as confirmed by the water contact angle test and FTIR analysis. The FDR value depends on the structural properties of the membrane including porosity and pore size as well as on the membrane hydrophilicity. As presented in Table 3, the M4 membrane had a smaller pore size in comparison with the chemically cross-linked membranes. The membrane with narrow pores has more fouling tendency due to pore blocking and accumulation of the oil droplets on the membrane surface; therefore, the flux decline is more serious for the M4 membrane.

The membrane fouling in the microfiltration process is a combination of the pore blocking as irreversible resistance and the formation of a layer of oil droplets on the membrane surface as reversible resistance [36]. The values of the mass transport resistances in Table 6 show the cake resistance that

Table 5
The separation performance of some membranes in the separation oil/water emulsion

Membrane	Oil concentration in feed (ppm)	Flux (kg/(m² h))	Oil rejection (%)	Process	Ref.
M1	3,000	4,104	95.0	Microfiltration	This study
M2	3,000	1,118	99.4	Microfiltration	
M3	3,000	390	99.5	Microfiltration	
M4	3,000	1,163	99.8	Microfiltration	
PVA coating on PVA nanofibers	1,350	60.8	99.5	Ultrafiltration	[3]
PVA/TiO_2 nanofibers	3,000	4,047	99.9	Microfiltration	[11]
Polyether-block-amide (PEBAX) on PVA nanofibers	1,350	130	99.8	Ultrafiltration	[25]
Polyethersulfone (PES)/TiO_2	3,000	8	99.9	Ultrafiltration	[29]
PVA nanofibers	1,350	130	99.5	Ultrafiltration	[31]
PVA coating on PAN nanofibers	1,500	250	99.5	Ultrafiltration	[32]
Polyvinyl acetate (PVAc)-coated nylon 6/Silica nanofibers	1,000	4,814*	99.2	Microfiltration	[33]
PA6(3)T nanofibers	250	44.3	92.7	Microfiltration	[34]

*Pure water flux.

Table 6
The flux decrease ratio and mass transport resistances of various prepared membranes

Membrane	R_M (×10¹⁰/m)	R_F (×10¹⁰/m)	R_C (×10¹⁰/m)	R_T (×10¹⁰/m)	FDR (%)
M1	4.80	2.80	6.60	14.20	42.09
M2	5.54	6.77	42.10	54.41	81.34
M3	7.10	30.00	110.00	147.10	91.10
M4	13.4	13.7	27.5	54.60	79.31

is due to the deposition and accumulation of oil drops on the surface of the membrane, which was the dominant resistance against the permeation through the membrane. Similar results have been observed by other researchers [37,38]. Since the membrane fouling due to the cake/gel layer formation on the membrane surface is reversible fouling, the fouled electrospun PVA membranes can be cleaned and reused by an appropriate washing procedure.

4. Conclusion

In this work, the photo and chemically cross-linked electrospun PVA nanofiber membranes were prepared and employed for the separation of oil from the synthetic oil/water emulsion. In addition, the chemical and physical properties as well as the separation and antifouling performance of the membranes were examined in detail. The main findings of this study may be summarized as follows:

- Addition of C=C bonds to PVA not only changes PVA chemically but also alerts the physical properties of the resultant electrospun nanofiber membrane.
- The SEM analysis revealed the fact that the UV-cross-linked PVA membrane possesses finer fibers in comparison with the chemically cross-linked membranes.
- For the chemically cross-linked nanofiber membranes, the cross-linking reaction occurred between the polymer fibers and the fibers fused together during the thermal treatment.
- The swelling test indicated that as the cross-linking agent increased the swelling degree decreased.
- The permeation fluxes for the chemically cross-linked membranes decrease in the order of M1 < M2 < M3 due to a decrease in the pore size and hydrophilicity of the membranes.
- The analysis of the mass transport resistances indicated that the cake resistance was the dominant resistance. Since this type of membrane fouling is a reversible fouling, the fouled electrospun PVA membranes can be cleaned and reused by an appropriate washing procedure.
- Although the photo-cross-linked PVA nanofiber membrane had a higher oil rejection, on the contrary, it suffered from its poor antifouling behavior in comparison with the other specimens.

Symbols

A — Membrane area, m²
C_f — Oil concentration in the feed, ppm
C_p — Oil concentration in the permeate, ppm
D_p — Mean pore diameter, m
FDR — Flux decrease ratio, %
J_{oi} — Initial oil/water flux, kg/m² h
J_{of} — Final steady-state oil/water flux, kg/m² h

J_{wf} — Pure water flux of fouled membrane, kg/m² h
J_{wv} — Pure water flux of virgin membrane, kg/m² h
ΔP — Operating pressure, MPa
Q — Pure water permeate flow rate, m³/s
R — Oil rejection, %
R_c — Cake resistance, 1/m
R_f — Fouling resistance, 1/m
R_m — Membrane resistance, 1/m
SD — Degree of swelling, %
t — Time duration of microfiltration experiment, h
W — Weight of collected permeate, g
W_d — Membrane weight at dry state, g
W_w — Membrane weight at wet state, g

Greek letters

δ — Membrane thickness, m
ε — Bulk porosity
η — Water viscosity, Pa·s
ρ — Water density, g/m³

References

[1] A. Ahmad, N. Yusuf, B. Ooi, Preparation and modification of poly (vinyl alcohol) membrane: effect of crosslinking time towards its morphology, Desalination, 287 (2012) 35–40.
[2] B. Bolto, T. Tran, M. Hoang, Z. Xie, Crosslinked poly (vinyl alcohol) membranes, Prog. Polym. Sci., 34 (2009) 969–981.
[3] Z. Tang, J. Wei, L. Yung, B. Ji, H. Ma, C. Qiu, K. Yoon, F. Wan, D. Fang, B.S. Hsiao, UV-cured poly (vinyl alcohol) ultrafiltration nanofibrous membrane based on electrospun nanofiber scaffolds, J. Membr. Sci., 328 (2009) 1–5.
[4] W.S. Lyoo, J.H. Youk, S.W. Lee, W.H. Park, Preparation of porous ultra-fine poly (vinyl cinnamate) fibers, Mater. Lett., 59 (2005) 3558–3562.
[5] P. Gupta, S.R. Trenor, T.E. Long, G.L. Wilkes, In situ photo-cross-linking of cinnamate functionalized poly (methyl methacrylate-co-2-hydroxyethyl acrylate) fibers during electrospinning, Macromolecules, 37 (2004) 9211–9218.
[6] Y. Ertas, T. Uyar, Cross-linked main-chain polybenzoxazine nanofibers by photo and thermal curing; stable at high temperatures and harsh acidic conditions, Polymer, 84 (2016) 72–80.
[7] A. Klymenko, T. Nicolai, C. Chassenieux, O. Colombani, E. Nicol, Formation of porous hydrogels by self-assembly of photo-cross-linkable triblock copolymers in the presence of homopolymers, Polymer, 106 (2016) 152–158.
[8] T. Uhlich, G. Tomaschewski, H. Komber, Synthesis of a hydrophobised and photocrosslinkable prepolymer based on poly(viny1 alcohol), React. Funct. Polym., 28 (1995) 55–60.
[9] J. Zeng, H. Hou, J.H. Wendorff, A. Greiner, Photo-induced solid-state crosslinking of electrospun poly (vinyl alcohol) fibers, Macromol. Rapid Commun., 26 (2005) 1557–1562.
[10] B. Zeytuncu, S. Akman, O. Yucel, M.V. Kahraman, Synthesis and adsorption application of in situ photo-cross-linked electrospun poly(vinyl alcohol)-based nanofiber membranes, Water Air Soil Pollut., 226 (2015) 173–192.
[11] E. Karimi, A. Raisi, A. Aroujalian, TiO2-induced photo-cross-linked electrospun polyvinyl alcohol nanofibers microfiltration membranes, Polymer, 99 (2016) 642–653.
[12] F. Chen, J.W. Hayami, B.G. Amsden, Electrospun poly (l-lactide-co-acryloyl carbonate) fiber scaffolds with a mechanically stable crimp structure for ligament tissue engineering, Biomacromolecules, 15 (2014) 1593–1601.
[13] J.F. Li, Z.L. Xu, H. Yang, C.P. Feng, J.H. Shi, Hydrophilic microporous PES membranes prepared by PES/PEG/DMAc casting solutions, J. Appl. Polym. Sci., 107 (2008) 4100–4108.
[14] A.D. Eaton, M.A.H. Franson, Standard Methods for the Examination of Water and Wastewater, American Public Health Association, Washington, 2005.
[15] E. Mahmoudi, L.Y. Ng, M.M. Ba-Abbad, A.W. Mohammad, Novel nanohybrid polysulfone membrane embedded with silver nanoparticles on graphene oxide nanoplates, Chem. Eng. J., 277 (2015) 1–10.
[16] D.E. Heath, J.J. Lannutti, S.L. Cooper, Electrospun scaffold topography affects endothelial cell proliferation, metabolic activity, and morphology, J. Biomed. Mater. Res. A, 94 (2010) 1195–1204.
[17] J.W. Rhim, H.B. Park, C.S. Lee, J.H. Jun, D.S. Kim, Y.M. Lee, Crosslinked poly (vinyl alcohol) membranes containing sulfonic acid group: proton and methanol transport through membranes, J. Membr. Sci., 238 (2004) 143–151.
[18] X. Xu, J.-F. Zhang, Y. Fan, Fabrication of cross-linked polyethyleneimine microfibers by reactive electrospinning with in situ photo-cross-linking by UV radiation, Biomacromolecules, 11 (2010) 2283–2289.
[19] B. Ding, H.Y. Kim, S.C. Lee, C.L. Shao, D.R. Lee, S.J. Park, G.B. Kwag, K.J. Choi, Preparation and characterization of a nanoscale poly (vinyl alcohol) fiber aggregate produced by an electrospinning method, J. Polym. Sci. B, 40 (2002) 1261–1268.
[20] C.M. Hassan, N.A. Peppas, Structure and morphology of freeze/thawed PVA hydrogels, Macromolecules, 33 (2000) 2472–2479.
[21] J. Gohil, P. Ray, Polyvinyl alcohol as the barrier layer in thin film composite nanofiltration membranes: preparation, characterization, and performance evaluation, J. Colloid Interface Sci., 338 (2009) 121–127.
[22] A.K. Sonker, N. Tiwari, R.K. Nagarale, V. Verma, Synergistic effect of cellulose nanowhiskers reinforcement and dicarboxylic acids crosslinking towards polyvinyl alcohol properties, J. Polym. Sci., 54 (2016) 2515–2525.
[23] A.K. Sonker, K. Rathore, R.K. Nagarale, V. Verma, Crosslinking of polyvinyl alcohol (PVA) and effect of crosslinker shape (aliphatic and aromatic) thereof, J. Polym. Environ., 26 (2018) 1782–1794.
[24] J. Mulder, Basic Principles of Membrane Technology, Springer Science & Business Media, Dordrecht, Netherlands, 2012.
[25] X. Wang, X. Chen, K. Yoon, D. Fang, B.S. Hsiao, B. Chu, High flux filtration medium based on nanofibrous substrate with hydrophilic nanocomposite coating, Environ. Sci. Technol., 39 (2005) 7684–7691.
[26] R.L. Mauck, B.M. Baker, N.L. Nerurkar, J.A. Burdick, W.-J. Li, R.S. Tuan, D.M. Elliott, Engineering on the straight and narrow: the mechanics of nanofibrous assemblies for fiber-reinforced tissue regeneration, Tissue Eng. B, 15 (2009) 171–193.
[27] K. Masoudnia, A. Raisi, A. Aroujalian, M. Fathizadeh, Treatment of oily wastewaters using the microfiltration process: effect of operating parameters and membrane fouling study, Sep. Sci. Technol., 48 (2013) 1544–1555.
[28] I. Sadeghi, A. Aroujalian, A. Raisi, B. Dabir, M. Fathizadeh, Surface modification of polyethersulfone ultrafiltration membranes by corona air plasma for separation of oil/water emulsions, J. Membr. Sci., 430 (2013) 24–36.
[29] V. Moghimifar, A. Raisi, A. Aroujalian, Surface modification of polyethersulfone ultrafiltration membranes by corona plasma-assisted coating TiO2 nanoparticles, J. Membr. Sci., 461 (2014) 69–80.
[30] K. Masoudnia, A. Raisi, A. Aroujalian, M. Fathizadeh, A hybrid microfiltration/ultrafiltration membrane process for treatment of oily wastewater, Desal. Wat. Treat., 55 (2015) 901–912.
[31] X. Wang, D. Fang, K. Yoon, B.S. Hsiao, B. Chu, High performance ultrafiltration composite membranes based on poly (vinyl alcohol) hydrogel coating on crosslinked nanofibrous poly (vinyl alcohol) scaffold, J. Membr. Sci., 278 (2006) 261–268.
[32] K. Yoon, B.S. Hsiao, B. Chu, High flux ultrafiltration nanofibrous membranes based on polyacrylonitrile electrospun scaffolds and crosslinked polyvinyl alcohol coating, J. Membr. Sci., 338 (2009) 145–152.
[33] M.S. Islam, J.R. McCutcheon, M.S. Rahaman, A high flux polyvinyl acetate-coated electrospun nylon 6/SiO2 composite microfiltration membrane for the separation of oil-in-water emulsion with improved antifouling performance, J. Membr. Sci., 537 (2017) 297–309.

[34] Y.M. Lina, G.C. Rutledge, Separation of oil-in-water emulsions stabilized by different types of surfactants using electrospun fiber membranes, J. Membr. Sci., 563 (2018) 247–258.
[35] S.M. Thompson, L.M. Masukawa, D.A. Prince, Temperature dependence of intrinsic membrane properties and synaptic potentials in hippocampal CA1 neurons in vitro, J. Neurosci., 5 (1985) 817–824.
[36] B. Chakrabarty, A. Ghoshal, M. Purkait, Cross-flow ultrafiltration of stable oil-in-water emulsion using polysulfone membranes, Chem. Eng. J., 165 (2010) 447–456.
[37] A. Rahimpour, S. Madaeni, A. Taheri, Y. Mansourpanah, Coupling TiO2 nanoparticles with UV irradiation for modification of polyethersulfone ultrafiltration membranes, J. Membr. Sci., 313 (2008) 158–169.
[38] A. Razmjou, J. Mansouri, V. Chen, The effects of mechanical and chemical modification of TiO2 nanoparticles on the surface chemistry, structure and fouling performance of PES ultrafiltration membranes, J. Membr. Sci., 378 (2011) 73–84.